Energy 171 (2019) 205–217

Contents lists available at ScienceDirect

Energy

journal homepage: www.elsevier.com/locate/energy

A realistic model for battery state of charge prediction in energy management simulation tools

Bart Homan [a, b, *], Marnix V. ten Kortenaar [b], Johann L. Hurink [a], Gerard J.M. Smit [a]

[a] Computer Architecture for Embedded Systems, University of Twente, Enschede, the Netherlands
[b] Dr Ten B.V., Wezep, the Netherlands

ARTICLE INFO

Article history:
Received 24 July 2018
Received in revised form
28 November 2018
Accepted 18 December 2018
Available online 23 December 2018

Keywords:
Pb-acid battery
Li-poly battery
LiFePo battery
State-of-Charge
Prediction
Energy management

ABSTRACT

In this paper, a comprehensive model for the prediction of the state of charge of a battery is presented. This model has been specifically designed to be used in simulation tools for energy management in (smart) grids. Hence, this model is a compromise between simplicity, accuracy and broad applicability. The model is verified using measurements on three types of Lead-acid (*Pb-acid*) batteries, a Lithium-ion Polymer (*Li-Poly*) battery and a Lithium Iron-phosphate (*LiFePo*) battery. For the Pb-acid batteries the state of charge is predicted for typical scenarios, and these predictions are compared to measurements on the *Pb-acid* batteries and to predictions made using the KiBaM model. The results show that it is possible to accurately model the state of charge of these batteries, where the difference between the model and the state of charge calculated from measurements is less than 5%. Similarly the model is used to predict the state of charge of *Li-Poly* and *LiFePo* batteries in typical scenarios. These predictions are compared to the state of charge calculated from measurements, and it is shown that it is also possible to accurately model the state of charge of both *Li-Poly* and *LiFePo* batteries. In the case of the *Li-Poly* battery the difference between the measured and predicted state of charge is less than 5% and in the case of the *LiFePo* battery this difference is less than 3%.

1. Introduction

Batteries have become an important attribute of future energy systems [1]. Examples include using a battery (1) for emergency situations, (2) to store electricity generated by *photo-voltaic panels* (PV-panels) during the day for usage during the night, and (3) to store electricity at times it is cheap for usage at times it is expensive. Furthermore, to get insight in the working of future energy systems, more simulations are used for example to predict weak points in existing grids [2], to investigate the effect of increasing infeed of renewable energy, or to explore the possibility of new types of grids [3]. To be able to accurately estimate the energy usage and power flows in a grid for such simulations, accurate models are needed for all relevant devices connected to the grid, including batteries.

To describe the behavior of batteries a whole set of models and methods are available. Many of these models and methods are suitable for *state of charge* (SoC) estimation [4], but most of these are only suitable for one specific type of battery, for example lead-acid (*Pb-acid*) [5,6]. For *Pb-acid* batteries, some of these models are even very accurate. The *Schiffer-model* [7] for instance is very accurate, and takes most physio-chemical processes that occur in the battery (corrosion, acid stratification, gassing) into account. However, this model requires solving of a large number of equations and (estimated) values for 28 different parameters, many of which are only available to the manufacturers of the battery. The *Kinetic Battery Model* (KiBaM) introduced by Manwell et al. [8] takes less phenomena into account, and can predict the SoC using only 3 parameters, making use of non-linear equations. Other models that yield high accuracies for the SoC prediction, like the *Husnayin method* [9] make use of elaborate algorithms and require extensive computations and large data sets to be able to learn how to predict the state of charge of a particular battery. Also for lithium-ion polymer batteries (*Li-Poly*) many models are available for prediction of the state of charge [10]. For example the *Dualfoil model* [11] is very accurate, but also very complex to use, as the model requires over 50 input parameters to model the behavior of a *Li-Poly* battery, whereby again much of the needed information may only be available to the developers or manufacturers of the battery. The *Thevenin model*, a type of equivalent circuit model, can be used to

* Corresponding author. Tel. +31 53 489 28 93.
E-mail address: b.homan@utwente.nl (B. Homan).

https://doi.org/10.1016/j.energy.2018.12.134

predict the SoC of *LiFePo* batteries, see e.g. Refs. [12,13], the model is considered very reliable, however the model parameters are difficult to determine and the model itself complex to use [14]. A more generally applicable method is the *Coulomb counting method* [15], which can be used to estimate the state of charge of any battery based on measurements. This method can produce highly accurate values for the prediction of the current state of charge, but does not provide a prediction of a future state of charge based on the planned actions applied to the battery.

Within the context of smart grids and energy management, the state of the grid and the relevant assets in the near future (e.g the SoC of a battery) as e.g. energy plans have to be submitted to markets a day ahead and deviations are penalized [16]. With the increasing amount of flexibility in batteries (both domestic batteries and those found in electric vehicles), such market mechanisms are also becoming increasingly interesting in the residential sector (see e.g. the design of the universal smart energy framework [17]). Hence, in order to optimize the operation of a smart grid, a scalable and model-predictive control approach is required to benefit from the opportunities provided by these flexible assets in the near future. One example of such a control approach is given by Gerards et al. [18], who introduce the Profile Steering algorithm to devise a power consumption plan in a scalable way for a cluster of devices. The heart of this approach are computational efficient device level planning algorithms which already exist for buffers (including batteries) [19] and electric vehicles [20]. However, the presented approaches utilize an ideal battery model (similar to coulomb counting), and thus they do not take battery voltage into account. Therefore, the predicted energy and power that the battery can provide may be estimated overly optimistic, resulting in deviations from the planning in reality. A model is needed that can accurately predict the future SoC while maintaining a low level of complexity to make it applicable for simulations of clusters of hundreds/thousands of distributed battery systems.

An existing simpler model for for battery State of Charge prediction is the Diffusion Buffer model[1] (DiBu-model) [21,22]. It has been developed to facilitate sufficiently accurate State of Charge (SoC) predictions, while being simple enough to be used within decentralized energy management tools like e.g. the *TRIANA* [23,24] and *DEMKit* [25,26] smart grid modelling environments.

The DiBu-model can be used to predict the effect of a sequence of actions (charging or discharging the battery) for several intervals in the future on the state of charge of a battery. Moreover the DiBu-model is more general, meaning that it has been designed to simulate the behavior of various battery types. It is based on a model for the prediction of the SoC in thermal energy storages, developed by van Leeuwen et al. [27]. The idea of the DiBu-model is first described in Ref. [21], where the similarities between thermal energy storage and electrical energy storage are discussed, and the first version of the model is presented. Also some difficulties and problems of the model are pointed out. In Ref. [22] these problems are addressed, and an improved model is presented. Also first results of the predictive capabilities of the model are presented. This paper adds a broad analysis of the predictive capabilities of the DiBu-model and a demonstration of its applicability on various types of batteries.

In Section 2 the DiBu-model is briefly explained, and it is shown how the relevant parameters can be determined from battery measurements. In Section 3 the batteries and measurement devices used in the research are described. The predictive capabilities of the DiBu-model are demonstrated by predictions of the state of charge (Section 4.1) of three different *Pb-acid* batteries during various charge, discharge and idle steps. In Section 4.2 improvements to the SoC predictions are discussed. The wide applicability of the DiBu-model is shown in Section 4.3, where the model is applied to a Lithium-ion Polymer (*Li-Poly*) and a Lithium Iron-phosphate (*LiFePo*) battery. Conclusions of all findings are included in all subsections of Section 4, and a general conclusion on all results is given in Section 5. Lastly the scope of possible future work is discussed in Section 6.

2. A comprehensive model for battery SoC prediction

The model proposed in Refs. [21,22] predicts the *state of charge* (SoC) in a future point in time (t), as a percentage of the maximum capacity (E_{max}) in Wh, based on the SoC at the current time (t-1). More precisely the state of charge (SoC_t), given as a fraction of the battery capacity, is calculated by adding the change of the SoC during time interval [t-1,t] to the previous SoC (SoC_{t-1}). The change of the SoC is based on the current (I_t) and voltage (U_t) in that time interval Δt between t-1 and t. In detail we have:

$$SoC_t = SoC_{t-1} + \frac{U_t \cdot I_t \cdot \Delta t}{E_{max}} \tag{1}$$

To calculate the SoC at some time T (SoC_T) starting from an initial SoC at time 0 (SoC_{start}) we need to know E_{max} and the current (I_t) and voltage (U_t) used during the time intervals [t-1,t], $t = t_{start} \ldots T$. The current (I_t) corresponds to what is applied to or demanded from the battery in the time interval. To calculate the voltages we consider four states of the battery: discharging (2a), idle time after discharging (2b), charging (2c) and idle time after charging (2d). For each of these four states, a different expression is used to determine the voltage. The basic formulas for these expressions are as follows. (The used parameters α, β, γ, δ, U_{max} t_0^* and SoC_{s0} are explained later.)

$$U_t = U_{t-1} + \frac{\alpha \cdot I_{t-1}}{SoC_{s0}} \tag{2a}$$

$$U_t = U_{t_0^*} + \left(U_{max} - U_{t_0^*}\right) \cdot \left(1 - e^{-\frac{t - t_0^*}{\beta \cdot \left(t - t_0^*\right) + \gamma}}\right) \tag{2b}$$

$$U_t = U_{t-1} + \frac{I_{t-1}}{\delta} \tag{2c}$$

$$U_t = U_{t-1} \tag{2d}$$

In Fig. 1, a schematic representation of the battery voltage during charge, discharge and idle steps is given.[2] When the battery is discharged Equation (2a) is used, in which the voltage (U_t) is calculated from the used current (I_t) in time interval [t-1,t], a constant α and the state of charge at the beginning of the discharge step (SoC_{s0}). When the battery is idle, after a discharging step, Equation (2b) applies, in which the voltage (U_t) is calculated from the voltage at the beginning of the idle step ($U_{t_0^*}$), the starting time of the idle step (t_0^*), the maximum voltage the battery can reach (U_{max}) and constants β and γ. When the battery is charged, Equation (2c) applies, in which the voltage (U_t) is calculated based on the used current (I_t) and a constant δ. When the battery is idle after

[1] The name Diffusion Buffer model for battery SoC prediction was chosen because the idea for this model came from a model designed to estimate the SoC of a heat-buffer.

[2] In order to keep the model as simple as possible, not all physical and chemical processes that can occur in a battery have been taken into account. Justifications for (most of) these choices have been discussed in previous publications, [21,22].

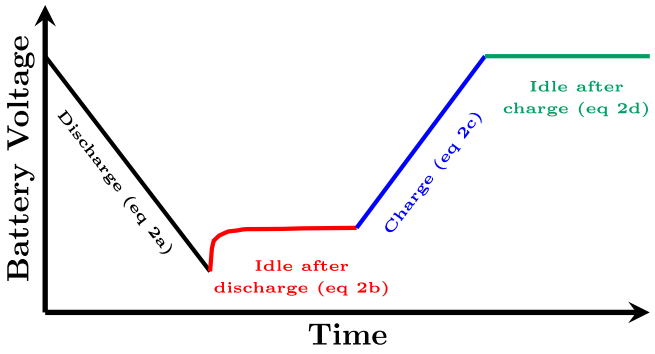

Fig. 1. Schematic representation of the battery voltage during charge, discharge and idle steps.

charging, Equation (2d) is used. For Equations (2b) and (2d) it is assumed that the idle time is short enough so that there are no self-discharge effects.

Estimates for the parameters α, β, γ and δ can be determined dependent on battery type, using e.g. the least-squares method on voltage measurements during the charging and discharging of the battery with a constant current [21]. The measurements necessary to determine the parameters α, β, γ and δ are outlined in Refs. [21,22]. Typical measurements to determine the parameters, and some example results are given in Fig. 2. The value of parameters α and δ are the slopes of the linear part of a constant current discharge curve (see Fig. 2a) and a constant current charge curve (see Fig. 2b) respectively. Multiple measurements, using various charge and discharge currents are used to determine values for α and δ to ensure accuracy. Note that the behaviour of the voltage during the constant current discharge of a battery is not completely linear (see Fig. 2a). However, in the model a linear approximation is made. When the battery is discharged with higher discharge currents the resulting discharge curve is diverging more form a linear curve. This behaviour is illustrated in Fig. A.1, in the appendix, which shows voltages during the constant current discharge of a typical lead acid battery with various discharge currents. This implies that the prediction of the voltage of the battery during discharging is less accurate when the discharge current is higher.

To determine the values of parameters β and γ, voltage measurements with two consecutive discharge steps and an idle period in between are used, see Fig. 2c. The voltage measured during the idle period, however, is not the real battery voltage but the *open circuit potential* (OCP). In practice the OCP is always higher than the discharge voltage, but here we can use the progression of the OCP in time, to determine the voltage at the start of the second discharge step. Again, multiple measurements are done using various discharge currents and idle periods to determine accurate values for the parameters. In a final step the parameters are once more verified by comparing the state of charge calculated from the measurements (SoC^{meas}) and the state of charge calculated using the DiBu-model (SoC^{DiBu}). In the presented case the difference between the SoC^{meas} and the SoC^{DiBu} is hardly visible and the maximum difference is calculated as 0.48%, (See Fig. 2d).

3. Materials and methods

In the following the measurements on lead-acid batteries are performed using a Vencon UBA5 battery analyzer [28], under standard conditions. The Vencon UBA 5 battery analyzer has a voltage accuracy of ± 0.2% and a current accuracy of ± 0.5%. The measurements on *Li-Poly* and *LiFePo* batteries are done on a Cadex

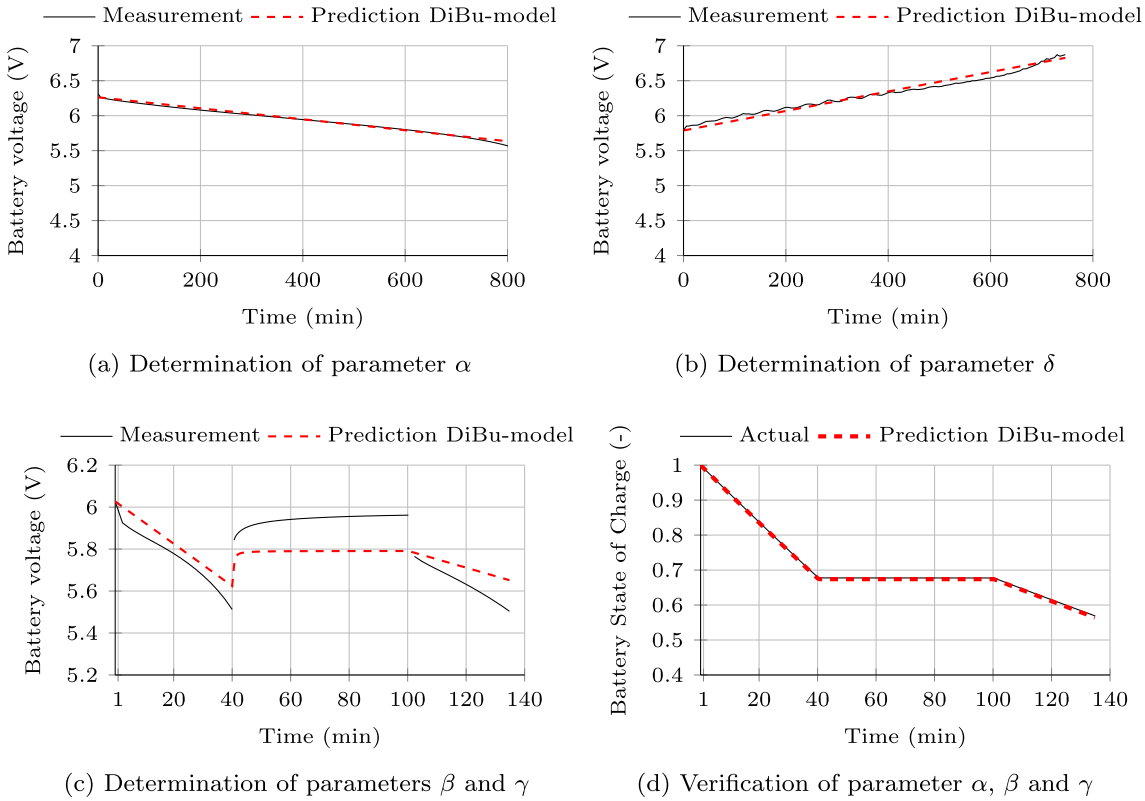

(a) Determination of parameter α

(b) Determination of parameter δ

(c) Determination of parameters β and γ

(d) Verification of parameter α, β and γ

Fig. 2. Measurements used in the determination of parameters α, β, γ and δ for lead-acid battery. Note that the actual SoC in Fig. 2d is calculated from voltage and current measurements.

C8000 battery analyzer [29], under standard conditions. Both the Vencon UBA5 (see Fig. A.2a) and the Cadex C8000 (see Fig. A.2b) battery analyzer are multi-purpose devices, used to measure the voltage, current and temperature, and to provide the load and charge. Using either device a sequence of charging, discharging and resting steps can be programmed, the analyzer then executes these steps and records the applied current and resulting voltage and temperature. The Cadex C8000 battery analyzer has a voltage accuracy of ± 0.1% and a current accuracy of ±0.25%. The parameters α, β, γ and δ, as well as the parameters necessary for the application of the KiBaM model are determined using the results of at least four separate measurements on the relevant battery. The lead-acid batteries used for this work are commercially available. The *Conrad* battery, is a Conrad CP672 valve regulated lead acid battery, the *Yuasa* battery is a Yuasa NP7-6 valve regulated lead acid battery and the *Multipower* battery is a MP7-6S lead-acid battery. The *Li-Poly* and *LiFePo* batteries are Dan-energy batteries, also commercially available. All measurements are carried out within safe operating limits (voltage, current and temperature) as supplied by the battery-manufacturer to ensure that the batteries are not damaged.

4. Results & discussion

In the following we first determine for the three lead-acid (*Pb-acid*) batteries the parameters presented in Section 2 using the model and method outlined also in that section. The three tested batteries have more or less the same specifications, but are made by different manufacturers; *Conrad*, *Yuasa* and *Multipower*, (the batteries are referred to by these names.) The achieved results are presented in Table 1. For all three tested batteries, the values for the parameters α, β, γ and δ respectively are very similar. The one exception to this is the γ value for the *Multipower* battery, which is three times smaller than the γ value for the other two batteries, the reason for this deviation is not yet clear. Using the parameters in Table 1, the DiBu-model given by formulas (1) and (2), is applied to predict the behaviour of the *Conrad*, *Yuasa* and *Multipower* batteries in a typical scenario. The voltage and SoC of each battery are predicted during consecutive charge, discharge and idle steps. The applied currents for each step in the scenario are given in Table 2.

The prediction of the voltage is not the main goal of the DiBu-model, but a necessary step in the SoC prediction. Therefore only one example of this step is presented. In Fig. 3 the measured and predicted voltage of the *Conrad* battery, under the applied currents is shown. The pattern of the predicted voltage, resembles the pattern of the measured voltage, however, the difference between the predicted and measured voltage is up to 0.54 V (or 7.7% of the maximum voltage) which seems to be quite large. Furthermore the difference between the prediction and the measurement is largest in discharging steps (*Step 5 and 9*) where the battery is discharged with 1 A, and 0.8 A respectively. However, as the goal of this model is not to give an accurate prediction of the battery voltage, but rather give an accurate prediction of the SoC this deviation of the voltage on its own is not directly an issue. Therefore, in the next section we investigate the SoC predictions in more detail.

Table 1
Characteristics and parameters determined for the three tested lead-acid batteries.

	Conrad	Yuasa	Multipower
Rated capacity (Ah)	7,2	7,0	7,0
Nominal voltage (V)	6,0	6,0	6,0
α (V/A)	3030×10^{-5}	3756×10^{-5}	4618×10^{-5}
β (−)	0,268	0249	0,218
γ (min)	2684	2323	0,839
δ (A/V)	2438×10^{4}	1727×10^{4}	1055×10^{4}

4.1. SoC predictions

The prediction for the state of charge for each of the three batteries is displayed in Fig. 4. In this figure, the predicted SoC is compared to the SoC calculated directly from measurements on each of the three batteries, by means of the Coulomb counting method [15]. Furthermore the SoC predicted with the DiBu-model is also compared to the SoC predicted using the *KiBaM model*. The KiBaM model or Kinetic Battery Model is a well known and often used model for the prediction of the SoC of lead-acid batteries [8]. The parameters used for the predictions in Fig. 4 are included in Table A.1. The differences between SoC^{meas} and SoC^{DiBu} and SoC^{KiBaM}, respectively, for al steps of the three tested batteries are included in Table 2. Note that the SoC differences included in the Tables A.2, A.3, A.4 and A.5 as well as those mentioned in the text are absolute differences between SoC's, expressed in percentage of the maximum SoC.

Fig. 4a shows the measured and predicted SoC of the *Conrad* battery. At the start, the SoC predicted with the DiBu-model (SoC^{DiBu}) deviates only slightly from the measured SoC (SoC^{meas}): from the start of the experiment to the end of *Step 8* (t ~ 1100 min), the maximum difference between the SoC^{DiBu} and the SoC^{meas} is 2.6%. During *Step 9*, however, the deviation between the SoC^{DiBu} and the SoC^{meas} doubles to 5.1%. From step *Step 10* onward the deviation increases slowly, reaching a maximum difference between the SoC^{DiBu} and the SoC^{meas} of 12.1% at the end of *Step 14*. The SoC predicted using the KiBaM model (SoC^{KiBaM}) starts out with a slight, increasing deviation. From the start of the experiment to *Step 12* at t ~ 1400 min, the SoC^{KiBaM} is less accurate than the SoC^{DiBu}. From *Step 12* onward however, SoC^{KiBaM} is slightly more accurate than the SoC^{DiBu}.

The measured and predicted SoC of the *Yuasa* battery are shown in Fig. 4b. From the start of the experiment to the end of *Step 8* (t ~ 1250 min), there is only a slight difference between the SoC^{DiBu} and the SoC^{meas}: the maximum difference in this time interval is 1.5%. The difference increases to 8.4% over the three discharge steps that follow. In the last charge step (*Step 14*), the difference between the SoC^{DiBu} and the SoC^{meas} increases slightly, to 8.5% at the end of the experiment. From the start of the experiment, until the middle of *Step 10* (t ~ 1400 min), the SoC^{KiBaM} is less accurate than the SoC^{DiBu}. During the following discharge steps the SoC^{KiBaM} is more accurate than the SoC^{DiBu}. During the final charging step (*step 14*) the SoC^{KiBaM} again becomes less accurate than the SoC^{DiBu}. Moreover, over-all the SoC^{DiBu} is more accurate than the SoC^{KiBaM}.

The SoC predicted for the *Multipower* battery compared to the measured SoC, both shown in Fig. 4c, behave in much the same way as was the case for the *Conrad* and *Yuasa* batteries. However, where the differences between SoC^{DiBu} and SoC^{meas} for the *Conrad* and *Yuasa* batteries strongly increase during *Step 9*, for the *Multipower* battery it does not. The difference between the SoC^{DiBu} and the SoC^{meas} is small (1.9%) at the start of the experiment, during the experiment it slowly increases to 9.7% at the end of the final step (*Step 14*). From the start of the experiment, the SoC^{KiBaM} is slightly more accurate than the SoC^{DiBu}. During *Steps 10–13* the SoC^{DiBu} is more accurate than the SoC^{KiBaM}, and in the final step *Step 14* the SoC^{KiBaM} is more accurate again. The SoC^{DiBu} and SoC^{KiBaM} are very similar in this case, the absolute difference between the two is never more than 0.9%.

A second scenario has been explored where the *Conrad* battery is cyclically charged and discharged. The battery is charged with 400 mA for 8 h, and discharged with −400 mA for 8 h, between the charge and discharge steps the battery is idle for 30 min. The applied currents for each step in the scenario are given in Table 3. Fig. 5 shows the measured and the predicted SoC using the DiBu-model and the KiBaM model during this scenario.

Table 2
The charge, discharge and idle steps used in the experiments described in Figs. 3 and 4. To protect the batteries a maximum cut-off voltage of 6.9 V and minimum cut-off voltage of 5.5 V was set. In some steps the cut-off voltage was reached before the step was completed; in these instances the real charge or discharge step length, displayed in Figs. 3 and 4 is shorter than indicated in this table.

Step #	Type	Current (A)	Length (min)	Total (min)	Step #	Type	Current (A)	Length (min)	Total(min)
1	Charge	0.4	420	420	8	Charge	0.2	240	1455
2	Idle	0	15	435	9	Discharge	−0.8	240	1695
3	Discharge	- 0.5	60	495	10	Idle	0	30	1725
4	Idle	0	30	525	11	Discharge	−0.5	240	1965
5	Discharge	- 1.0	60	585	12	Idle	0	15	1980
6	Charge	0.4	600	1185	13	Discharge	−0.1	600	2580
7	Idle	0	30	1215	14	Charge	0.4	600	3180

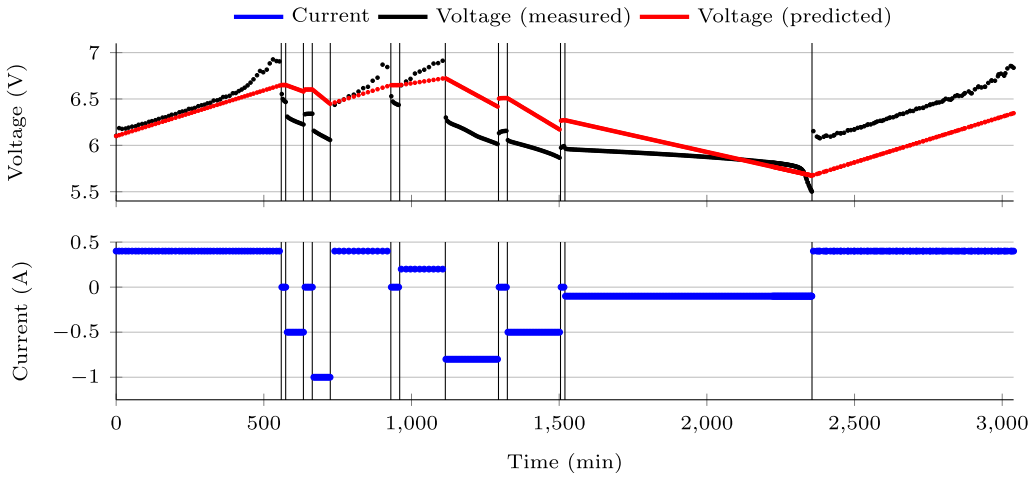

Fig. 3. The applied current and resulting voltage during a the test on the *Conrad* battery. The black vertical lines represent the moment of step-change.

In the first cycle the SoC^{DiBu} matches the SOC^{meas} closely, the largest deviation in this cycle is 3.2%, which occurs at the end of *Step 3*, the discharge step. During the second cycle the difference between SOC^{meas} and SoC^{DiBu} remains mostly constant during *Step 4, 5, 6* and then doubles to 6.4% at the end of the discharge step, *Step 7*. The third cycle shows again an increase (to 9.7%) in the deviation between SOC^{meas} and SoC^{DiBu} in the discharge step (*Step 11*). So the deviation between SOC^{meas} and SoC^{DiBu} is progressively worse in consecutive cycles, and in this scenario the deviation increases mainly during the discharge steps. The SoC^{KiBaM} already shows a 3.3% deviation from the SoC^{meas} after the first step. The deviation between SOC^{meas} and SoC^{KiBaM} is also progressively worse in consecutive cycles but the deviation increases during the charge steps (*Step 1, 5, 9*, and remains constant during the other steps. In this scenario the SoC predicted using the DiBu-model is always more accurate than the SoC predicted using the KiBaM model. The deviations between the SOC^{meas} and SoC^{DiBu} or SoC^{KiBaM} for each step have been included in Table A.3 in the appendix.

In a different publication [30] the DiBu-model has also been used to predict the SoC of more realistic scenarios, than those presented in Figs. 4 and 5. Comparisons between the SoC^{DiBu} and the SoC^{meas} (in Fig. 6 of that publication) show that the predictions made using the DiBu model match reality very well. The difference between the SoC^{DiBu} and the SoC^{meas} is generally less than 1.5%.

From the experiments on the *Conrad*, *Yuasa* and *Multipower* batteries, outlined in Tables 2 and 3 and shown in Figs. 3–5 it can be concluded that:

- The accuracy of the SoC^{DiBu} is very good in the first 1000 min of both experiments, having a maximum difference to SoC^{meas} of only 2.5% in the first experiment, and 3.2% in the second.
- The accuracy of the SoC^{DiBu} deteriorates after 1000 min, leading to a maximum difference between the SoC^{DiBu} and the SoC^{meas} of 12.1% in both experiments.
- The SoC^{DiBu} prediction for discharge steps is less accurate than for charge steps.
- The level of accuracy of the SoC^{DiBu} is comparable to the level of accuracy of the SoC^{KiBaM}. Generally, in charging steps the SoC^{DiBu} is more accurate than the SoC^{KiBaM}, while the reverse is true in the discharging steps.

4.2. Improvements of the SoC prediction

The state of charge at time t is predicted using the measured values for the voltage and current at time t-1. In each consecutive step of the state of charge prediction, the values predicted for the previous time step are used as input. Although the SoC prediction of one single time step ($\Delta t = 30$ s) produces only a very small error, the SoC predicted over a longer period of time requires many consecutive predictions and in each of the consecutive predictions the error accumulates, so the total error may increase and become considerable. In the previous experiments we choose to predict the state of charge over long periods up to 3400 min (i.e. 57 h, or 6800 steps of Δt) in advance. In the experiments the SoC^{DiBu} deviated at most 2.5% from the SoC^{meas} in the first 1000 min, after which the accuracy of the SoC^{DiBu} started deteriorating. This implies that, in this experiment the accuracy of the state of charge prediction using the DiBu-model is only of a high quality when the prediction horizon is not too long. Based on these insights, in a practical setting, the starting values for the battery voltage (U_t) and state of charge (SoC_t) should be calibrated after some period of time based on

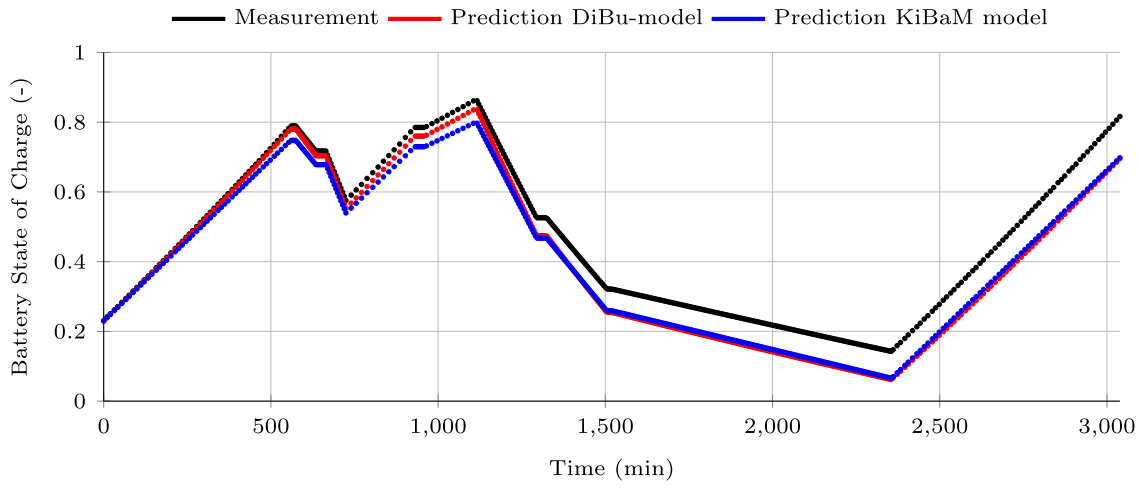

(a) SoC of the *Conrad* battery.

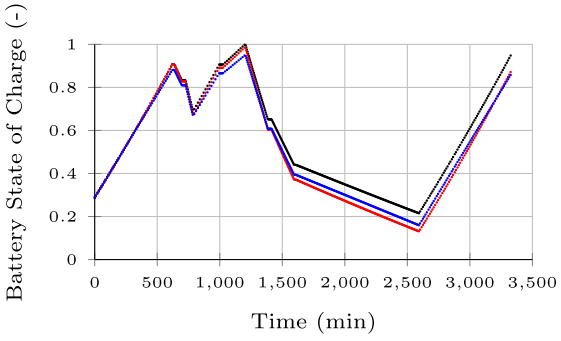

(b) SoC of the *Yuasa* battery.

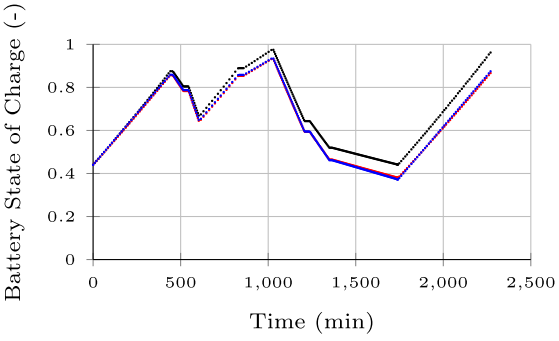

(c) SoC of the *Multipower* battery.

Fig. 4. State of Charge of selected batteries (see Table 1), calculated from measurements on the batteries compared to predictions using the DiBu-model and the KiBaM model.

Table 3
The charge, discharge and idle steps used in the cyclic charging/discharging experiment described in Fig. 5.

Step #	Type	Current (A)	Length (min)	Total (min)	Step #	Type	Current (A)	Length (min)	Total(min)
1	Charge	4	480	480	7	Discharge	−4	480	2010
2	Idle	0	30	510	8	Idle	0	30	2040
3	Discharge	−4	480	990	9	Charge	4	480	2520
4	Idle	0	30	1020	10	Idle	0	30	2550
5	Charge	4	480	1500	11	Discharge	−4	480	3030
6	Idle	0	30	1530					

measurements or other indications for the values of (U_t) and (SoC_t) achieved at the time of calibration. These standard techniques should improve the accuracy of the prediction for the next time interval. It was also observed that the inaccuracy of the SoC^{DiBu} increased during the discharging steps, in particular when a high discharging current was applied. Therefore, it is suggested that for improving the accuracy in a practical setting, the starting values for the battery voltage (U_t) and state of charge (SoC_t) should be updated after each discharging step. Using these improvements the maximum prediction horizon is limited to the time of one full charge/discharge cycle. Moreover, the inaccuracy caused by a discharge step is corrected immediately after this step, so the overall accuracy should improve.

Note that if the DiBu-model is used as part of a (smart) grid simulation, updating the starting values for (U_t) and (SoC_t) effectively shortens the maximum time over which the SoC^{DiBu} can be predicted. However, if the DiBu-model is used to predict the behaviour of an actual battery, for example when using model-predictive control, measurements on that battery can be used to update the starting values for (U_t) and (SoC_t). In practice, battery management hardware (e.g. the Victron Multiplus [31]) is almost always involved when a battery is used in a (smart) grid environment. It is common for such a device to measure the battery voltage and current, and determine the actual SoC from these measurements. It is also common for these devices to recalibrate the SoC determination when the battery is either completely full or completely empty. The measured voltage, and/or determined SoC can be used freely to update the (U_t) and state of charge (SoC_t) to increase the accuracy of the prediction.

Based on the results up to now a scenario for possible improvements has been explored: the starting values for (U_t) and (SoC_t) are calibrated at the beginning of a step that starts after a

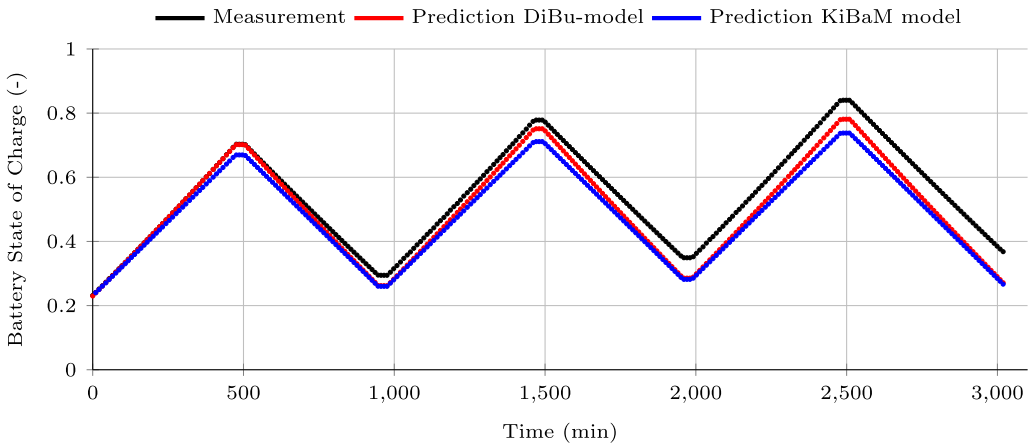

Fig. 5. State of Charge of the *Conrad* battery, during cyclic charging/discharging, calculated from measurements compared to predictions using the DiBu-model and the KiBaM model.

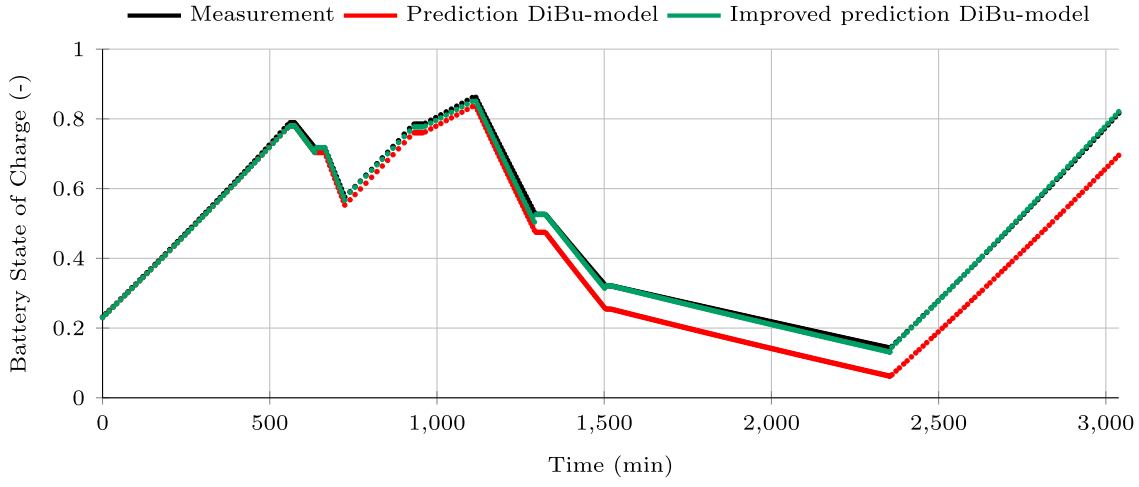

(a) SoC of the *Conrad* battery.

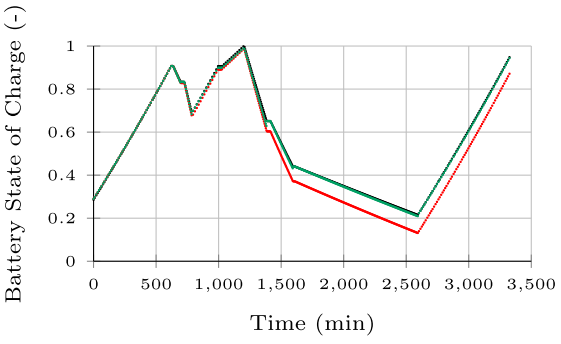

(b) SoC of the *Yuasa* battery.

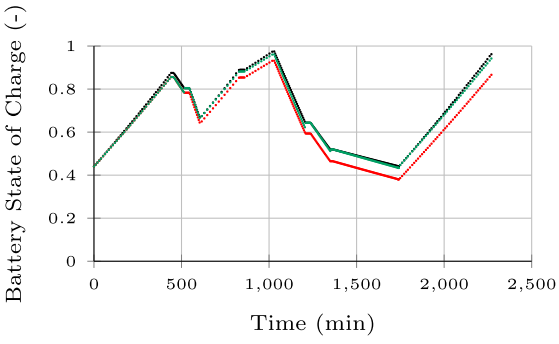

(c) SoC of the *Multipower* battery.

Fig. 6. Comparison of the measured SoC and SoC predicted using the DiBu-model for the three batteries, updating the SoC_{start} and V_{start} at the end of each discharge step, or updating the SoC_{start} and V_{start} at the ending of a step, after some specific time intervals. Note that in some intervals the green lines (representing the improvements) completely overlap the black line (representing the measurement) making these lines difficult to distinguish from each other. (For interpretation of the references to colour in this figure legend, the reader is referred to the Web version of this article.)

discharge step, i.e. at the beginning of *Steps 4, 6, 10, 12 and 14*. The results of these experiments are shown in Fig. 6. The deviations between the SoC^{DiBu} predicted without improvements, and the SoC^{DiBu} predicted using the improvements for all steps of the three tested batteries are included in Table A.4.

Fig. 6a displays the SoC^{meas} and SoC^{DiBu} for the *Conrad* battery with and without the suggested improvements. If the improvements are applied, the difference between SoC^{meas} and SoC^{DiBu} at

the end of the experiment is reduced to 0.5%. This is a significant improvement to the original experiment, but can be attributed mainly to the fact that the update occurred just before the start of the last step (*Step 14*). However, the maximum difference between SoC^{meas} and SoC^{DiBu} during the whole experiment is reduced to 2.8%, which occurs at the end of *Step 9*. The difference between SoC^{meas} and SoC^{DiBu} for the *Yuasa* battery, (see Fig. 6b) at the end of the experiment is 0.5%, which is, again a significant improvement to the original experiment, but again that is caused by the update at the beginning of *Step 14*. The difference is small over the entire course of the experiment, staying below 1.3% except for the last part of step *Step 9* where the difference increases to 2.7% within 30 min. When the improvements are applied on the SoC predictions for the *Multipower* battery, (see Fig. 6c) similar improvements are observed. The difference between SoC^{meas} and SoC^{DiBu} at the end of the experiment is reduced to 2.1%. The maximum difference between the SoC^{meas} and SoC^{DiBu} is reduced from 9.7% to 2.6% over all, where the maximum difference occurs during the last 30 min of *Step 9*. Note that improvements also could be applied to the predictions done with the KiBaM model. It is to be expected that the accuracy of SoC^{KiBaM} is improved if the starting values of U_t and SoC_t are calibrated after each discharge step. However this has not been explored further in this work.

From the improved experiments on the *Conrad*, *Yuasa* and *Multipower* batteries, shown in Fig. 6 it can be concluded that:

- The accuracy of the State of Charge predicted using the DiBu-model can be improved when the time over which the prediction is made is shortened, i.e. if the starting values of U_t and SoC_t are calibrated after a certain amount of time.
- The accuracy of the State of Charge predicted using the DiBu-model can be improved when the values for U_t and SoC_t are calibrated after a discharge step.

4.3. Verification with additional battery types

To demonstrate the wider applicability of the DiBu-model, the model is also applied on Lithium-ion Polymer (*Li-Poly*) and Lithium Iron-phosphate (*LiFePo*)[3] batteries. The parameters of these batteries, listed in Table 4, were determined using the method outlined in Section 2. It was determined from the measurements that even though the *capacity recovery effect* is present in both *Li-Poly* and *LiFePo* batteries, its effects for the DiBu-model are minimal (see Fig. A.3). The voltage where the second discharge starts is almost identical to the voltage where the first discharge ends, even after an idle step of 1 h. For the model this means that the voltage remains constant during idle steps after discharging, hence the parameters β and γ are both zero.

4.3.1. Lithium-ion polymer batteries

The behaviour of the Li-Poly battery was investigated for a typical scenario, during a set of consecutive charge, discharge and idle steps. The characteristics of the different steps, are outlined in Table 5. Note that this scenario is not the same as the test scenario for the *Pb-acid* batteries, this is the result of limitations of the battery and testing equipment.

In Fig. 7 the SoC calculated from measurements, and the predicted SoC for the *Li-Poly* battery are displayed. The pattern of SoC^{DiBu} follows closely the pattern of SoC^{meas} but the difference increases over time. The largest difference between SoC^{DiBu} and SoC^{meas} is 4.3%, reached at the start of *Step 16*. In *Steps 1 through 15* the maximum difference between SoC^{DiBu} and SoC^{meas} is 2.1%, which is reached at the end of *Step 10*. After *Step 17* the difference between SoC^{DiBu} and SoC^{meas} increases in the discharge steps and decreases somewhat in the charge steps. The difference between the SoC^{DiBu} and SoC^{meas} for all steps has been included in Table A.5.

As mentioned the increase in difference between SoC^{DiBu} and SoC^{meas} is largest in the discharge steps. At the end of (discharge) *Steps 12, 16 and 21* the difference is 1.7%, 4.3% and 3.9% respectively. At the end of charge steps that follow these discharge steps, namely *Steps 15, 19 and 22*, the difference is 0.9%, 1.3% and 3.3%, which is a reduction in all cases. This behaviour matches the behaviour observed for the lead-acid batteries (Section 4.1). The SoC^{DiBu} can be improved if the values for U_t and SoC_t are calibrated after each discharge step, as proposed in Section 4.2. The green line in Fig. 7 shows the SoC^{DiBu} if these improvements are applied. In this case the aforementioned differences in *Steps 12, 16 and 21* are greatly reduced. However, the largest difference (4.8%) is now located in *Step 10* and is larger than the largest difference without the improvements applied. This is caused by an overestimation of the SoC in that step. On the whole, however, the difference between SoC^{DiBu} and SoC^{meas} is smaller when the improvements are applied. The difference between the SoC^{DiBu}, with and without the improvements, for all steps is presented in Table A.5.

Table 4
Characteristics and parameters determined for the *Li-Poly* and *LiFePo* test batteries.

	Li-Poly	LiFePo
Rated capacity (Ah)	5.2	4.5
Nominal voltage (V)	25.2	26.4
α (V/A)	2.834×10^{-4}	1.765×10^{-4}
β (−)	0	0
γ (min)	0	0
δ (A/V)	2.772×10^{4}	5.169×10^{4}

4.3.2. Lithium Ironphosphate batteries

The behaviour of the LiFePo batteries (see Table 4) was also investigated for a typical scenario, during a set of consecutive charge, discharge and idle steps. The characteristics of the different steps, are outlined in Table 6. Note, that again the scenario is not the same as the test scenario for the *Pb-acid* and *Li-Poly* batteries, this is again the result of limitations to the battery and testing equipment.

In Fig. 8 the SoC derived from measurements on the *LiFePo* battery (SoC^{meas}) and the predicted state of charge (SoC^{DiBu}) are shown. The difference between the SoC^{meas} and the SoC^{DiBu} increases progressively during the measurement, except during *Step 16*, where the difference deceases slightly. The largest difference between (SoC^{meas}) and (SoC^{DiBu}) is 11.6% and this indeed occurs at the end of the last step (*Step 23*). The difference increases most during the discharge steps, and remains mostly constant during the charge and idle steps (for the difference per step see Table A.5). If the improvements proposed in Section 4.2 are applied (the values for U_t and SoC_t are re-calibrated after *Steps 4,5,6,10,11,12,13,19,20 and 22*), the predictions improve. The corresponding SoC^{DiBu} is also shown in Fig. 8. When the improvements are applied, the largest difference between (SoC^{meas}) and (SoC^{DiBu}) is then 2.7%, and this occurs at the end of *Step 4*.

From the experiments on the *Li-Poly* and *LiFePo* batteries, outlined in Tables 4 and 5 and shown in Figs. 7 and 8 it can be concluded that:

- The capacity recovery effect is negligible for *Li-Poly* and *LiFePo* batteries, hence the parameters β and γ are both zero.

[3] Although LiFePo is used in this work as the abbreviation for Lithium Iron-phosphate, it's proper chemical formula is $LiFePO_4$.

Table 5
The charge, discharge and idle steps used in the experiment described in Fig. 7.

Step #	Type	Current (A)	Length (min)	Total (min)	Step #	Type	Current (A)	Length (min)	Total(min)
1	Idle	0	5	5	12	Discharge	−2.6	15	340
2	Charge	2	45	50	13	Idle	0	30	370
3	Charge	1.5	45	95	14	Charge	1.3	30	400
4	Idle	0	15	110	15	Charge	2.2 → 1.2	15	415
5	Discharge	−1.3	30	140	16	Discharge	−5.2	15	430
6	Idle	0	30	170	17	Idle	0	30	460
7	Discharge	−1.3	30	200	18	Charge	2	18.5	478.5
8	Charge	1.5	60	260	19	Charge	2.0 → 0.65	41.5	520
9	Charge	2	25	285	20	Idle	0	10	530
10	Charge	2.0 → 1.0	20	305	21	Discharge	−2.6	25	555
11	Discharge	−1.3	20	325	22	Charge	1.3	25	580

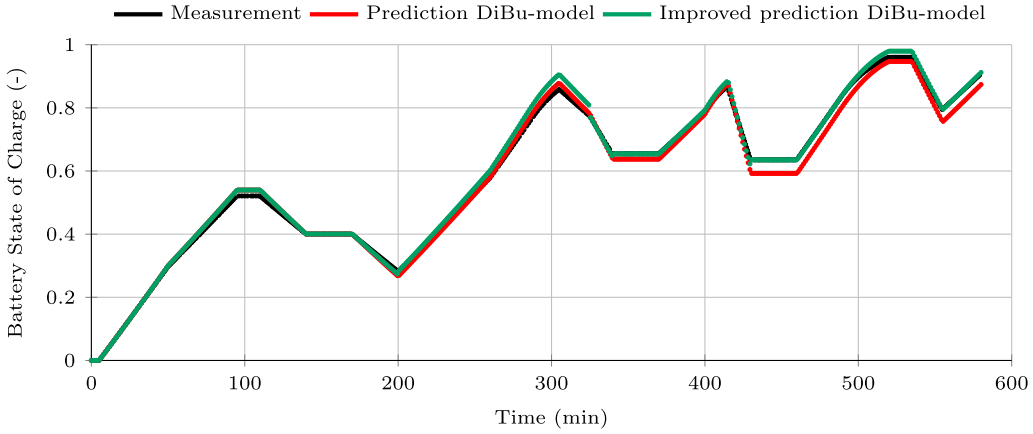

Fig. 7. State of Charge of the *Li-Poly* battery (see Table 4), calculated from measurements on the batteries, compared to predictions using the DiBu-model, and compared to predictions using the DiBu-model updating the SoC_{start} and V_{start} at the end of each discharge step.

Table 6
The charge, discharge and idle steps used in the experiment described in Fig. 8.

Step #	Type	Current (A)	Length (min)	Total (min)	Step #	Type	Current (A)	Length (min)	Total(min)
1	Charge	2	45	45	13	Discharge	−4	15	605
2	Charge	0.5	245	290	14	Idle	0	30	635
3	Idle	0	15	305	15	Charge	0.5	120	755
4	Discharge	−1	30	335	16	Charge	1	60	815
5	Discharge	−1.5	30	365	17	Charge	2	30	845
6	Discharge	−2	30	395	18	Idle	0	30	875
7	Charge	1.5	60	455	19	Discharge	−0.5	120	995
8	Charge	2	45	500	20	Discharge	−1	60	1055
9	Idle	0	15	515	21	Charge	0	15	1070
10	Discharge	−1	30	545	22	Discharge	−2	20	1090
11	Discharge	−2	25	570	23	Charge	1	120	1210
12	Discharge	−3	20	590					

- The DiBu model can be successfully used to predict the SoC of the tested *Li-Poly* and *LiFePo* batteries.
- For the *Li-Poly* battery the difference between SoC^{DiBu} and SoC^{meas} fluctuates over the various charge, discharge and idle steps. The difference remains quite small, the largest difference is 4.3%, at the end of *step 16*.
- For the *LiFePo* battery the difference between SoC^{DiBu} and SoC^{meas} progressively increases, reaching a difference between between SoC^{DiBu} and SoC^{meas} of 11.6% at the end of the experiment.
- For both battery types the difference between SoC^{DiBu} and SoC^{meas} increases most during the discharge steps.
- For both battery types the accuracy of the State of Charge prediction using the DiBu-model can be improved if the values for U_t and SoC_t are calibrated after each discharge step.

5. Conclusions

A simple yet accurate model for the prediction of the battery state of charge, the DiBu-model was proposed in Refs. [21,22]. This model was developed specifically for usage in tools for simulation, prediction and control of smart grids. As such the model yields accurate predictions of the state of charge, while being simple enough to apply in such tools. In this work the DiBu-model is applied to predict the state of charge of several different batteries. The model predicts the battery voltage during charging, discharging and idle periods, and based on these voltages the state of charge is predicted. To apply the model, first four parameters have to be determined from measurements on the battery in question. In a first step it has been shown that the DiBu-model can be used to accurately predict the behaviour of various lead-acid batteries. The difference between

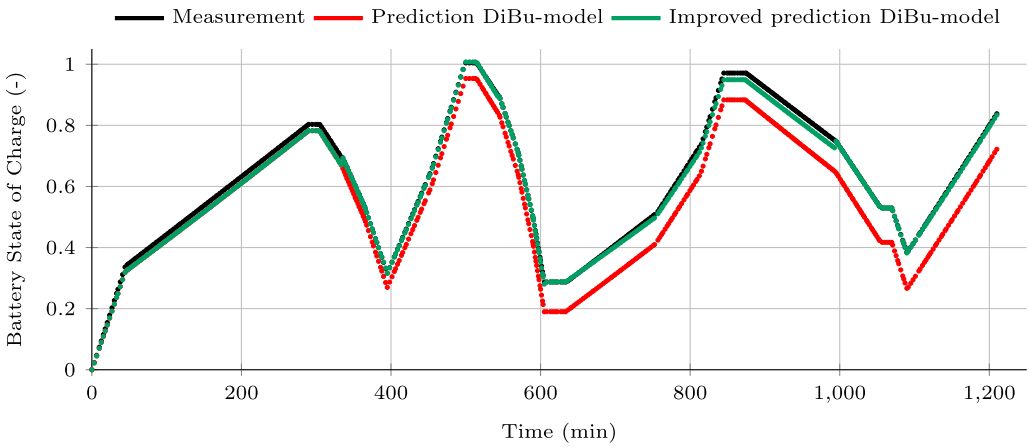

Fig. 8. State of Charge of the *LiFePo* battery (see Table 4), calculated from measurements on the batteries compared to predictions using the DiBu-model, and compared to predictions using the DiBu-model updating the SoC_{start} and V_{start} at the end of each discharge step.

Table 7
Average and maximum deviation between SoC^{meas} and SoC^{DiBu} off all experiments presented in Section 4.

SoC prediction	Corresponding		Average	Maximum	Occurs in
	Figure	Table	deviation (%)	deviation (%)	step #
Conrad	4a	2	5.7	12.1	14
Conrad - improvements	4a	2	0.7	2.8	9
Yuasa	4b	2	5.6	8.5	14
Yuasa - improvements	4b	2	0.5	2.7	9
Multipower	4c	2	4.6	9.7	14
Multipower - improvements	4c	2	0.8	2.6	9
Conrad 2	5	3	4.0	9.7	11
Li-Poly	7	5	1.7	3.9	22
Li-Poly - improvements	7	5	1.5	4.8	10
LiFePo	8	6	7.0	11.8	22
LiFePo - improvements	8	6	1.2	2.7	4

the state of charge predicted using the DiBu-model (SoC^{DiBu}), and the state of charge calculated from the measurements (SoC^{meas}) for all predictions has been summarised in Table 7.

For Pb-acid batteries, the difference between SoC^{DiBu} and SoC^{meas} has been shown to be less than 10% for a state of charge prediction over 3000 min (~ 50 h). It has also been shown that the accuracy of the state of charge predictions using the DiBu-model, is equal to, or in some cases better than the accuracy of state of charge predictions using the well established KiBaM model. However, the KiBaM model is more complicated and less suited for usage in tools for simulation, prediction and control of smart grids. Furthermore it has been shown that the DiBu-model also can be used to accurately predict the behaviour of Li-Poly and LiFePo batteries. In the case of the Li-Poly batteries the difference between SoC^{DiBu} and SoC^{meas} has been shown to be 4.3% for a state of charge prediction over 600 min (~ 10 h). In case of the LiFePo batteries the difference between SoC^{DiBu} and SoC^{meas} has been shown to be 11.6% for a state of charge prediction over 1200 min (~ 20 h). It has also been shown that the accuracy of the predictions can be improved by periodically updating the starting values for the battery voltage and state of charge.

6. Future work

Future work is dedicated to generalise the DiBu-model. One part of this is the verification of the DiBu-model for other battery types such as e.g. *Nickel-Cadmium* and *Nickel-Metalhydrate* batteries. Another part is the verification of the model for different load profiles, such as profiles where the battery operates near or on its operating limits, profiles where the battery operates well beyond or below room temperature, or profiles of real house-loads. The effectiveness of the improvements for reduction of the deviation between the predicted SoC and the SoC calculated from measurements should also be evaluated for the aforementioned load-profiles. Yet another topic for future work is the implementation of the DiBu-model in smart grid simulation software like e.g. TRIANA [23,24] or DEMKit [26].

Acknowledgements

The authors thank the Dutch national program Switch2-Smartgrids (project Smart Grid Evolution) and the Dutch organisation RVO for their support. The authors would also like to acknowledge the anonymous reviewers for their constructive comments on this work. Lastly the authors want to thank Richard van Leeuwen for his invaluable help in the inception of the DiBu-model.

Appendix A

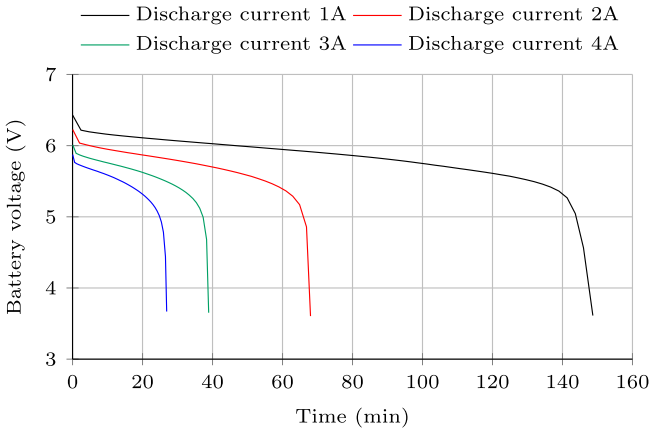

Fig. A.1. Typical behaviour of the battery voltage during discharge, with varying discharge currents, of a 6V 4 A h lead acid battery.

(a) Vencon UBA5 (b) Cadex C8000

Fig. A.2. The battery analysis equipment used to do the measurements and analyses in this work. As an example two of the Pb-acid batteries are connected to the Vencon UBA5 (A.2a) and a LiFePo battery is connected to the Cadex C8000 (A.2b).

Table A.1
Characteristics and parameters of the KiBaM model determined for the three test batteries.

	Conrad	Yuasa	Multipower
Rated capacity (Ah)	7.2	7.0	7.0
Nominal voltage (V)	6.0	6.0	6.0
C (As)	2.592×10^{-5}	2.520×10^{-5}	2.520×10^{-5}
k' (−)	0.664	1.105	0.211
c (−)	0.013	0.008	0.050

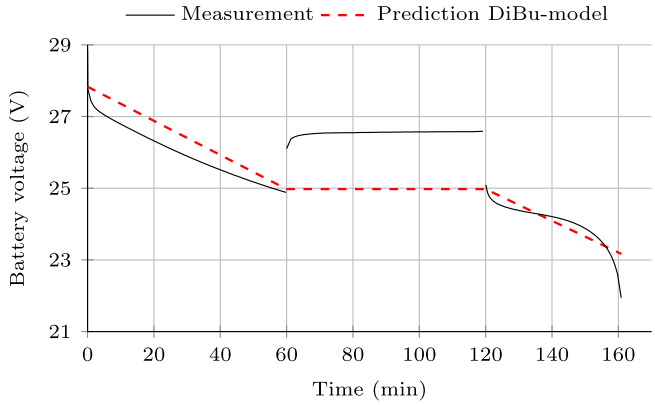

Fig. A.3. Example of the determination of parameters β and γ for the Li-Poly testing battery. The voltage at the end of the first discharge step (t = 60 min) is almost equal to the voltage at the beginning of the second discharge step (t = 120 min), hence β and γ are chosen such that the starting voltage of the second discharge step is predicted correctly, an the voltage behaviour during the idle step is ignored.

Table A.2
Maximum deviation between the predicted SoC and the SoC calculated from measurements (in %) for the *Conrad*, *Yuasa* and *Multipower* batteries. Corresponds to Fig. 4a, b and c.

Step #	Maximum deviation from measured value (%)					
	Conrad		*Yuasa*		*Multipower*	
	DiBu-model	KiBaM model	DiBu-model	KiBaM model	DiBu-model	KiBaM model
1	0.9	4.1	0.4	2.6	1.9	1.6
2	0.9	4.1	0.0	2.6	1.9	1.6
3	1.4	4.1	0.5	2.6	2.1	1.7
4	1.4	3.9	0.5	2.3	2.1	1.7
5	2.3	3.9	1.8	2.3	2.5	2.0
6	2.5	5.5	1.8	4.1	3.6	3.2
7	2.5	5.5	1.5	4.1	3.6	3.2
8	2.6	6.5	1.5	5.1	4.3	4.1
9	5.1	6.5	4.8	5.1	5.,0	4.8
10	5.1	5.8	4.8	4.3	5.0	4.8

(*continued on next page*)

Table A.2 (*continued*)

Step #	Maximum deviation from measured value (%)					
	Conrad		*Yuasa*		*Multipower*	
	DiBu-model	KiBaM model	DiBu-model	KiBaM model	DiBu-model	KiBaM model
11	6.7	6.2	6.9	4.6	5.5	5.8
12	6.7	6.2	6.9	4.6	5.5	5.8
13	8.1	7.7	8.4	5.6	6.1	6.9
14	12.1	11.9	8.5	9.0	9.7	8.8

Table A.3
Maximum deviation between the predicted SoC and the SoC calculated from measurements (in %) for the charge / discharge cycle scenario for the *Conrad* battery. Corresponds to Fig. 5.

Step #	Maximum deviation from measured value (%)	
	DiBu-model	KiBaM model
1	0.2	3.3
2	0.1	3.3
3	3.2	3.4
4	3.2	3.4
5	3.2	6.7
6	2.7	6.7
7	6.4	6.7
8	6.4	6.7
9	6.4	10.2
10	5.9	10.2
11	9.7	10.2

Table A.4
Maximum deviation between the predicted SoC and the SoC calculated from measurements (in %) for the *Conrad*, *Yuasa* and *Multipower* batteries, applying the improvements. Corresponds to Fig. 6a, b and c.

Step #	Maximum deviation from measured value (%)					
	Conrad		*Yuasa*		*Multipower*	
	DiBu-model	Improvements	DiBu-model	Improvements	DiBu-model	Improvements
1	0.9	0.9	0.4	0.4	1.9	1.9
2	0.9	0.9	0.0	0.0	1.9	1.9
3	1.4	1.4	0.5	0.5	2.1	2.1
4	1.4	0.0	0.5	0.0	2.1	0.0
5	2.3	0.9	1.8	1.3	2.5	0.3
6	2.5	0.8	1.8	0.7	3.6	0.9
7	2.5	0.8	1.5	0.7	3.6	0.8
8	2.6	1.1	1.5	1.0	4.3	1.4
9	5.1	2.8	4.8	2.7	5.0	2.6
10	5.1	0.0	4.8	0.0	5.0	0.0
11	6.7	1.1	6.9	1.1	5.5	0.8
12	6.7	0.0	6.9	0.0	5.5	0.0
13	8.1	1.2	8.4	0.6	6.1	0.8
14	12.1	0.5	8.5	0.5	9.7	2.1

Table A.5
Maximum deviation between the predicted SoC and the SoC calculated from measurements (in %) for the *Li-Poly* and *LiFePo* batteries, applying the improvements. Corresponds to Figs. 7 and 8.

Step #	Maximum deviation from measured value (%)			
	Li-Poly		*LiFePo*	
	DiBu-model	Improvements	DiBu-model	Improvements
1	0.0	0.0	1.8	1.8
2	0.3	0.3	2.1	2.1
3	1.9	1.9	2.1	2.1
4	1.9	1.9	2.7	2.7
5	0.0	0.0	4.1	0.0
6	0.0	0.0	4.7	0.2
7	1.6	1.0	5.3	0.3
8	0.3	2.4	5.1	0.3
9	0.8	3.3	5.1	0.3
10	2.0	4.8	6.1	0.8
11	0.7	3.2	7.2	0.1

Table A.5 (*continued*)

Step #	Maximum deviation from measured value (%)			
	Li-Poly		*LiFePo*	
	DiBu-model	Improvements	DiBu-model	Improvements
12	1.7	1.1	8.4	0.1
13	1.7	0.0	9.7	0.7
14	0.7	0.6	9.7	0.0
15	0.9	1.9	9.8	1.1
16	4.3	2.5	9.4	1.8
17	4.3	0.0	8.8	2.2
18	3.6	0.1	8.8	2.2
19	1.3	2.0	10.1	2.5
20	1.3	2.0	11.2	0.0
21	3.9	0.1	11.2	0.0
22	3.3	0.6	11.8	0.3
23			11.6	0.4

List of abbreviations

Pb-acid	Lead acid
Li-Poly	Lithium-ion polymer
LiFePo	Lithium Iron-phosphate
PV-panels	Photo-voltaic panels
USEF	Universal Smart Energy Framework
OCP	Open Circuit Potential
SoC	State of Charge
SoC^{DiBu}	SoC predicted using the DiBu-model
SoC^{KiBam}	SoC predicted using the KiBam model
SoC^{meas}	SoC calculated from measurements
KiBam	Kinetic Battery model
DiBu-model	Diffusion Buffer model

References

[1] Roberts BP, Sandberg C. The role of energy storage in development of smart grids. Proc IEEE 2011;99:1139–44.
[2] Hoogsteen G, Molderink A, Hurink JL, Smit GJM, Schuring F, Kootstra B. Impact of peak electricity demand in distribution grids: a stress test. IEEE Powertech 2015;2015:1–6.
[3] Perez KX, Baldea M, Edgar TF, Hoogsteen G, van Leeuwen RP, van der Klauw T, Homan B, Fink J, Smit GJM. Soft-islanding a group of houses through scheduling of chp, pv and storage. In: IEEE energyconvol. 2016; 2016. p. 1–6.
[4] Chang W-Y. The state of charge estimating methods for battery: a review. ISRN Appl. Math. 2013:1–7.
[5] Jongerden MR, Haverkort BR. Which battery model to use? Softw. IET 2009;3:445–57.
[6] Dufo-López R, Lujano-Rojas JM, Bernal-Agustín JL. Comparison of different lead-acid battery lifetime prediction models for use in simulation of stand-alone photovoltaic systems. Appl Energy 2014;115:242–53.
[7] Schiffer J, Sauer DU, Bindner H, Cronin T, Lundsager P, Kaiser R. Model prediction for ranking lead-acid batteries according to expected lifetime in renewable energy systems and autonomous power-supply systems. J Power Sources 2007;168:66–78.
[8] Manwell JF, McGowan JG. Lead acid battery storage model for hybrid energy systems. Sol Energy 1993;50:399–405.
[9] Husnayain F, Utomo AR, Priambodo PS. State of charge estimation for a lead-acid battery using backpropagation neural network method. In: IEEE international conference on electrical engineering and computer science; 2014. p. 274–8.
[10] He H, Xiong R, Fan J. Evaluation of lithium-ion battery equivalent circuit models for state of charge estimation by an experimental approach. Energies 2011;4:582–98.
[11] Doyle M, Fuller T, Newman J. Modeling of galvanostatic charge and discharge of the lithium/polymer/insertion cell. J Electrochem Soc 1993;140:1526–33.
[12] Panchal S. Impact of vehicle charge and discharge cycles on the thermal characteristics of lithium-ion batteries. Master's thesis. 2014.
[13] Panchal S, Mcgrory J, Kong J, Fraser R, Fowler M, Dincer I, Agelin-Chaab M. Cycling degradation testing and analysis of a lifepo4 battery at actual conditions. Int J Energy Res 2017;41:2565–75.
[14] Hu X, Li S, Peng H. A comparative study of equivalent circuit models for li-ion batteries. J Power Sources 2012;198:359367.
[15] Ng KS, Moo CS, Chen YP, Hsieh YC. Enhanced coulomb counting method for estimating state-of-charge and state-of-health of lithium-ion batteries. Appl Energy 2009:1506–11.
[16] Koliou E, Eid C, Chaves-Ávila JP, Hakvoort RA. Demand response in liberalized electricity markets: analysis of aggregated load participation in the German balancing mechanism. Energy 2014;71:245–54.
[17] Universal smart energy framework, https://www.usef.energy, referenced 2017/12/20.
[18] Gerards MET, Toersche HA, Hoogsteen G, van der Klauw T, Hurink JL, Smit GJM. Demand side management using profile steering. In: 2015 IEEE eindhoven PowerTech; 2015. p. 1–6.
[19] van der Klauw T, Gerards MET, Hurink JL. Resource allocation problems in decentralized energy management. Spectrum 2017;39:749–73.
[20] van der Klauw T, Gerards MET, Smit GJM, Hurink JL. Optimal scheduling of electrical vehicle charging under two types of steering signals. In: IEEE PES innovative smart grid technologies, europe; 2014. p. 1–6.
[21] Homan B, van Leeuwen RP, Zhu L, de Wit JB, Smit GJM. Validation of a predictive model for smart control of thermal and electrical energy storage. In: IEEE energycon; 2016. p. 1–6.
[22] Homan B, van Leeuwen RP, ten Kortenaar MV, Smit GJM. A comprehensive model for battery state of charge prediction. IEEE Powertech 2017;2017:1–6.
[23] Molderink A, Bakker V, Bosman MGC, Hurink JL, Smit GJM. Management and control of domestic smart grid technology. IEEE Trans. Smart Grid 2010;1:109–18.
[24] Bakker V. Triana: a control strategy for smart grids. Ph.D. thesis. University of Twente; 2012.
[25] Hoogsteen G. Demkit: a flexible smart grid simulation and demonstration platform written in python. In: Hurink JL, Smit GJM, editors. Proceedings of the 'Energy-Open' workshop, WP 17-01. CTIT; 2017a. p. 26–7.
[26] Hoogsteen G. A cyber-physical systems perspective on decentralized energy management. Ph.D. thesis. University of Twente; 2017b.
[27] van Leeuwen R, Gebhardt I, de Wit J, Smit G. A predictive model for smart control of a domestic heat pump and thermal storage. In: SMARTGREENS; 2016. p. 1–10.
[28] UBA5 battery analyzer, http://www.vencon.com/product/uba5-battery-analyzer-charger/, referenced 2018/2/28.
[29] Cadex C8000 battery analyzer, http://www.cadex.com/en/products/c8000-battery-testing-system, referenced 2018/2/27.
[30] Homan B, Reijnders VMMJ, Hoogsteen G, Hurink JL, Smit GJM. Implementation and verification of a realistic battery model in the demkit simulation software. In: IEEE ISGT; 2018. p. 1–6.
[31] Victron Multiplus battery charger/inverter, https://www.victronenergy.com/inverters-chargers, referenced 2018/11/7.